euronoise
Naples 2003

Experimental and Computational Study of Unsteady Flow and Noise in a Lawnmower Casing

M.Bockhoff[a], K.Mones[a], S.Timouchev[b] K.Ilhichov[b]A.Aksenov[c]
[a]Centre Technique des Industries Mécaniques (CETIM), BP 80 067, 60 304 Senlis Cedex, France
[b]InteRe Co Ltd, 19 apt. 11 Engels St., 141400 Khimki, Russia
[c]TESIS, Moscow, Russia

In order to supply tools for low noise design to the manufacturers of lawnmowers CETIM has set up a research project on blade noise (which is predominant on medium size and big machines). Experimental studies are based on the use of a special test rig which allows to measure blade noise without disturbances from the drive unit and to determine simultaneously the pressure fluctuations generated by the blade. Numerical simulations using CFD software allow computation of the unsteady pressure field distribution inside the casing, identification of pseudo-sound perturbations near the blade and localisation of flow recirculation areas near to the casing outlet.

1. INTRODUCTION

Systematic measurements and source ranking, carried out on lawnmowers of various sizes with different types of drives (electric motors and combustion engines), have shown that blade noise becomes predominant on big machines (typically for cutting widths > 50 cm). This was the reason for setting up at CETIM a research project on blade noise, covering both , experimental studies and numerical simulations. The paper presents some details and first results of the project.

2. EXPERIMENTAL STUDIES

2.1 Blade test rig

A special test rig has been built in order to study the blade noise independently from engine noise and blade-deck interactions: **Figure 1**. The blade is driven by a silent electric motor, placed below the floor plate. A deck-engine assembly can be positioned above the blade without any direct, structural coupling. In addition, a circular segment of the floor plate , carrying 18 pressure transducers along a radius, can be rotated by small angular steps, in order to determine to the pressure field at the floor level: **Figure 1b**.

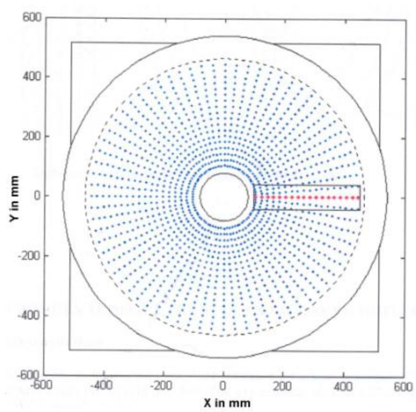

Figure 1: *Blade test rig, **(a)** general view* ***(b)*** *rotating floor plate with pressure gauges (red dots)*

2.2 Pressure distribution below the blade

Typical results obtained with this experimental set up are shown in **figure 2**. The left chart shows a rather week pressure field with almost no lift. The improved profile results in more lift, especially in the forward direction. The right chart illustrates negative influence of counterpressure which creates a very unregular pressure field and probably bad quality of cut.

Width of cut 41 cm, 3000 rpm, cutting hight 3 cm

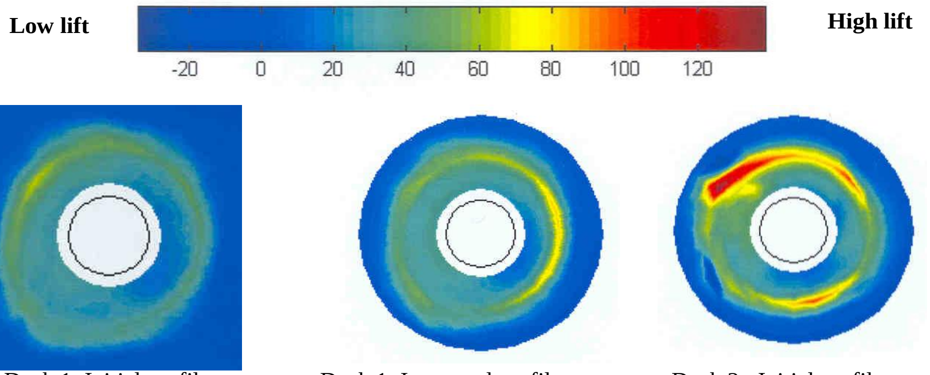

Deck 1: Initial profile
Free discharge

Deck 1: Improved profile
Free discharge

Deck 2: Initial profile
Discharge into grasscatcher

Figure 2: *Pressure field measured in the floor plane (lawnmower moves from left to right)*

2.3 Blade noise measurements

Systematic noise measurements have been made on the test rig under free field conditions by varying blade profile, blade-floor distance (cutting height) and rotation speed. **Figure 3** shows typical 1/3 octave sound power spectra obtained with a free running blade and with a blade-deck assembly. The difference of about 6 dBA, due to the aerodynamic blade-deck interaction, illustrates the necessity of a well designed deck profile for the noise reduction.

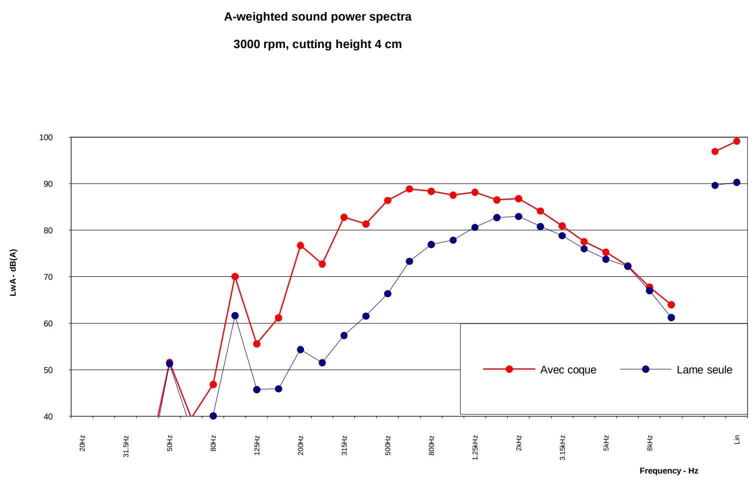

Figure 3: *Blade noise spectra, blade alone (blue), blade + deck (red)*

3. COMPUTATIONAL APPROACH

3.1 Governing equations

For prediction of airborne sound in the near field the mathematical model is based on a representation of fluctuating flow velocity field **V** as a combination of vortex and acoustic modes,

$$\mathbf{V} = \mathbf{U} + \nabla\varphi = \mathbf{U} + \mathbf{V_a}$$

Where

$\mathbf{U}$ - Velocity of transitional and rotational motion of incompressible liquid (vortex mode)

$\mathbf{V_a}$ - Velocity of pure deformation (acoustic mode)

φ - Acoustic potential

This gives acoustic-vortex wave equation relatively enthalpy oscillation in the isentropic flow of compressible fluid.

$$\frac{1}{a^2}\frac{\partial^2 i}{\partial t^2} - \Delta i = \nabla(\nabla(\tfrac{1}{2}U^2) - \mathbf{U}\times\zeta)$$

Right side of this equation represents the disturbing function, defined from the velocity field of vortex mode flow. It is determined from solution of unsteady equations of incompressible fluid with appropriate boundary conditions.

3.2 Numerical methods

For analysis of the problem 2-D code Harmony [1] and 3D code FlowVision [2] are used.

In 2D analysis vortex mode flow is computed in 2 steps. In the first step the flow around rotor is defined by discrete vortex method with applying “sliding-break-point” conditions on blades. In the second step unsteady Euler equations are solved for turbulent flow in the volute casing. Then disturbing function of the wave equation is defined from unsteady velocity field of the vortex mode. The computational procedure is the same as for centrifugal ventilators [3].

The 3D numerical procedure is based on non-staggered Cartesian grid with adaptive local refinement and a sub-grid geometry resolution method for description of curvilinear complex boundaries [1]. For vortex mode flow, unsteady Navier-Stokes equations are solved with applying k-ε turbulence model. Iterative procedure goes up to convergence to a periodical solution and subsequent definition of the disturbing function. Initial condition is zero pressure and velocity in entire computational domain. On rigid walls the logarithmic velocity profile is applied as a boundary condition for the turbulent flow. At the outer boundary free-outlet flow condition is used with linear extrapolation of velocity and pressure field from inner nodes.

Finally wave equation is solved relatively to pressure oscillation using an explicit numerical procedure. Zero pulsatory pressure is an initial condition for solution of wave equation. Casing and rotor walls are assumed absolutely rigid and infinite impedance is defined on all rigid walls. At the outer boundary the specific acoustic impedance equals unity.

3.3 results of 2D computation

2-Dimensional flow analysis is shown pseudo-sound perturbations due to intensive vortex creation on blade tips. Such a vortex sheets linked with blades are presented in **figure 4.**Wake zones rotating with blades create pressure fluctuations on blade passing frequency and its higher harmonics. It is found that intensity of wake zones essentially depends on blade shape and number of blades. It is shown that considerable reduction of pressure pulsation will be reached by changing a blade shape, number of blades and the volute radial gap.

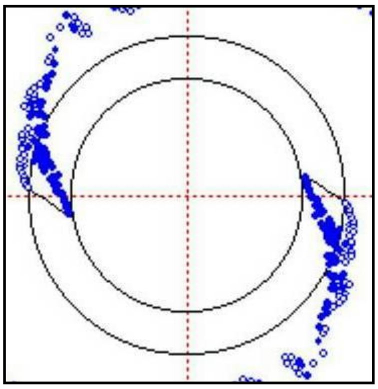

Figure 4: *Vortex sheet near blades*

The effect of such a changes is outlined in **figure 5** for two points in the volute casing.

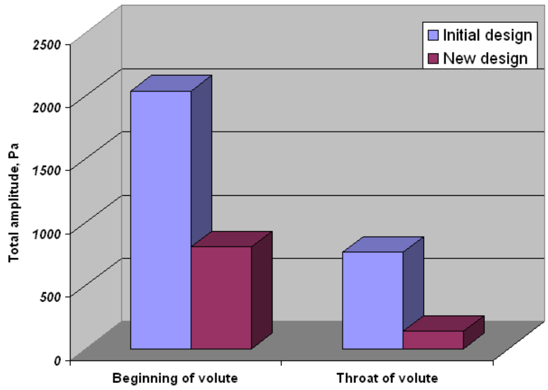

Figure 5: *Reduction of pressure pulsation accordingly 2D analysis*

These results show a big importance of optimal profiling of the fluid part of lawnmower to reduce noise level.

3.4 Results of 3D computation

Computational domain is a cylinder with diameter 1.5 m and height 0.75 m shown in **figure 6**.

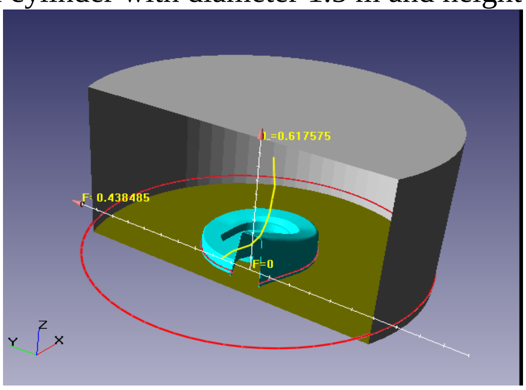

Figure 6: *Computational domain*

The bottom of the cylinder is considered as a rigid wall. Side and top surfaces are the outlet boundary.
Grid generation procedure produces a rectangular grid with local multilevel adaptation. The mesh will be automatically adapted in definite regions resulting in more accurate simulation. The original cell is divided into 8 equally size cells (1^{st} adaptation level). Furthermore the resulting cell can be divided again (2^{nd} adaptation level) and so up to the required level of accuracy.

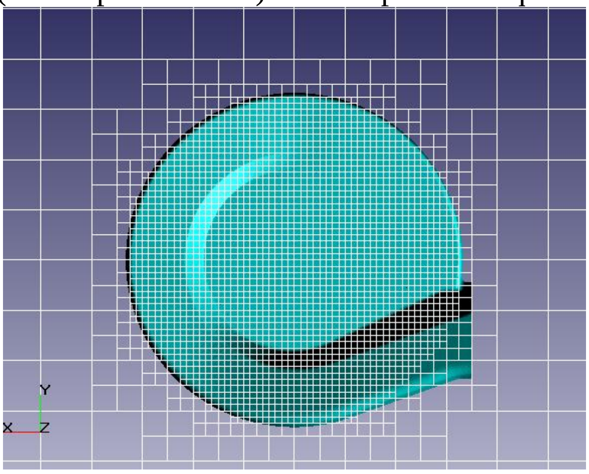

Figure 7: *Grid with local adaptation*

Sub-grid resolution method is used to approximate curvilinear geometry on the rectangular grid.
Let curvilinear boundary be represented by a set of plane facets (surface mesh). The sub-grid resolution method is used 'to fit' the Cartesian grid to the geometrical boundary in order to accurately describe the boundary conditions. The initial "parent" rectangular cell is cut off by the curvilinear surface and the parent cell is disjoined into a new more complex shape elements formed by the facet surface and the original grid cell faces.
Oscillatory part of the pressure field resulting from solution of wave equation in a certain time moment is presented in **figure 8**. The plane of this representation is shown in **figure 6** by a red circle section.

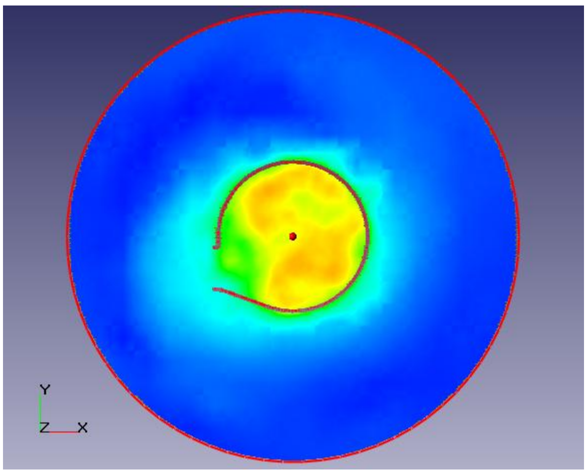

Figure 8: *Oscillation pressure field near the ground level*

One can see that the pressure field consists from a pseudo-sound zone in the volute casing and diffuse sound field near the lawn mower. Pseudo-sound oscillation generated directly by rotating blades and the amplitude here is equals to the pressure differential on the blade – about 1000 – 1500 Pa. Near field is created by unsteady fluid motion in vicinity of the casing, outlet air jet and recirculation, emission of sound waves from the exhaust section and from the gap between the casing and ground.

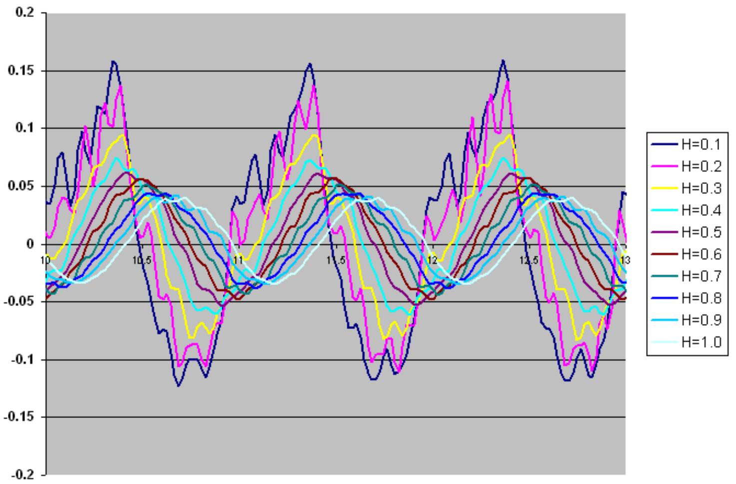

Figure 9: *Pressure signal on different distances*

The change of pressure signal near the outlet section is shown in **figure 9**. The pressure signal reduced by a fluid density multiplied by blade tip velocity squared. Location of points where signals are registered is outlined in **figure 6**. Points are uniformly distributed along the vertical line near the outlet section. On the plot, the H=0.1 corresponds to the lowest point and H=1.0 gives the top point.

One can see the pressure signal becomes more "sinusoidal" with attenuation of amplitude and change of phase. In the pseudo-sound zone (H=0.1—0.3) phases of signal are closely related.

4. CONCLUSION

New method for prediction of 3-dimensional near sound field in lawn mowers is developed on the base of acoustic-vortex representation.

REFERENCES

1. Timouchev S., Tourret J. Numerical Simulation of BPF Pressure Pulsation Field In Centrifugal Pumps. 19th International Pump Users Symposium, February 2002, Houston, Texas
2. Aksenov A.A., Dyadkin A.A., Gudzovsky A.V., 1996b, "Numerical Simulation of Car Tire Aquaplaning". Computational Fluid Dynamics '96, J.-A. Desideri, C.Hirsch, P.Le Tallec, M.Pandolfi, J.Periaux edts, John Wiley&Sons, pp. 815-820.
3. S. Timouchev Numerical Method And Software Package For Prediction Of Pressure Pulsation In Centrifugal Ventilators. Forum Acusticum'99 The 1st Joint Meeting of EAA and ASA, Berlin 14 - 19 March 1999